Effective dielectric response of polydispersed composites

Rubén G. Barrera
Instituto de Física, Universidad Nacional Autónoma de México, Apartado Postal 20-364,
01000 México, Distrito Federal, Mexico

Pedro Villaseñor-González
Instituto de Física, Universidad Autónoma de San Luis Potosí, 7800 San Luis Potosí, San Luos Potosí, Mexico

W. Luis Mochán
Laboratorio de Cuernavaca, Instituto de Física, Universidad Nacional Autónoma de México,
Aparatado Postal 139-8, 62190 Cuernavaca, Morelos, Mexico

Guillermo Monsivais
Instituto de Física, Universidad Nacional Autónoma de México, Apartado Postal 20-364,
01000 México, Distrito Federal, Mexico

We generalize the concept of renormalized polarizability introduced in a recently developed effective-medium theory to the case of polydispersed composites. We deal with a homogeneous and isotropic ensemble of spherical inclusions with a continuous distribution of sizes. The theory accounts for the correlated fluctuations among the induced dipole moments and the induced internal field within the long-wavelength dipolar approximation. The statistical properties of the ensemble enter in the final result through the two- and three-particle distribution functions. Numerical results are presented for a system of silver spheres in gelatin with a log-normal distribution of radii. The roles played by the dipolar fluctuations and by the size-dependent relaxation time, due to the surface scattering of the electrons, are analyzed and compared.

I. INTRODUCTION

The effect of the dispersion of sizes on the effective dielectric response of a composite has not been thoroughly examined even in the simplest case, which is the one that will be investigated here, of a homogeneous material with spherical inclusions located at random and with a given statistical distribution of radii. Besides the inherent importance of this problem, the lack of an accurate solution has also obstructed the very much needed comparison between the new effective-medium theories[1-16] and experiment.[17-28] While these theories are usually difficult to extend to an arbitrary distribution of radii, the experiments are commonly done in polydispersed samples. In the language of the electronic theory of random media the problem is to introduce diagonal disorder into theories which were tailored to deal with the non diagonal one, due to the long range of the electromagnetic interaction.

There are several size-dependent mechanisms which affect the polarizability of a single particle. For example, the dielectric function of a metallic inclusion, smaller than the electron mean free path in the bulk (~ 500 Å for silver) depends on its size due to the effects of the electron scattering with its surface.[29] Electron scattering may also be affected by size-dependent internal defects introduced during the process of preparation of the sample.[30] The dielectric response of even smaller particles (less than ~ 30 Å) will also differ from the one in the bulk, but now due to the discrete nature of the quantum levels of the conduction electrons when constrained into a small enough volume.[31] This effect is known as the quantum size effect, and it is obviously size dependent. On the other hand, large particles with radius of the order of the wavelength of light interact among themselves and with the external field through a scattering process which is also size dependent. Since this scattering process takes radiation away from the direction of the coherent beam, the concept of an effective dielectric response starts to lose its strict meaning[32] and it will not be discussed here any further.

In this paper we deal with medium-size inclusions (~ 30–300 Å) embedded in a homogeneous matrix. In particular, we consider a collection of spheres, with a given distribution of radii, such that retardation effects might be neglected and with filling fractions low enough so the dipolar approximation is sufficient. This problem has been treated, at least in the case of metallic spheres, by considering the effects of electron scattering with the surface or with internal defects of the spheres. This is usually done by introducing a radius-dependent relaxation time in the dielectric response of the conduction electrons for each of the spheres.[33] Here, we consider first that the dielectric function of the spheres ϵ_s is size independent. The effect that we want to isolate is the trivial dependence of the polarizability of the spheres with the cube of its radius. In this case, it is well known that the effects of polydispersion are completely absent in

         © 1990 The American Physical Society

mean-field theories. For example, in Maxwell-Garnett theory (MGT) the effective (or macroscopic) dielectric response ϵ_M is given through $(\epsilon_M - \epsilon_h)/(\epsilon_M + 2\epsilon_h) = f\tilde{\alpha}$, where ϵ_h is the dielectric function of the host material, f is the volume fraction of the particles, and $\tilde{\alpha} \equiv \alpha/a^3 = (\epsilon_s - \epsilon_h)/(\epsilon_s + 2\epsilon_h)$ is the effective polarizability α of a sphere with radius a divided by a^3, and is independent of a. Therefore the difference between the polydispersed and monodispersed composite will appear only in theories which go beyond mean field. In other words, the physical origin of the effect that we want to treat here comes from the correlated fluctuations among the induced dipole moments and the induced internal field.

The structure of theories which go beyond mean field is, in general, more complicated and an extension to include diagonal disorder is usually not straightforward. However, a simple effective-medium theory which contains the effect of the dipolar (or field) fluctuations has been recently developed.[15] In this theory the fluctuations are included by replacing in MGT the bare polarizability α by a renormalized one α^*. Since α^* has a clear physical interpretation, and its calculation is extremely simple, an extension to include diagonal disorder is entirely feasible. A first step in this direction has been already taken by considering a system with spheres of two different radii.[34] It was found that additional peaks appeared, in the imaginary part of the dielectric function of the composite as a function of frequency, due to the excitation of a richer spectrum of electromagnetic modes. Here we extend the concept of a renormalized polarizability to the case of an arbitrary dispersion of radii. We show results for the imaginary part of the effective dielectric function with a log-normal distribution of radii, for a system of silver spheres embedded in gelatin. First we assume that the dielectric function of the individual spheres are all identical. Then we repeat the calculation, but incorporating now the effects of surface scattering, and we compare both results. The paper is organized as follows: in Sec. II we develop the formalism and in Sec. III we present the numerical results comparing them with other approaches and with other effects. We illustrate the physical interpretation of the results by analyzing the case of a system of spheres with three different radii. Section IV is devoted to comments and conclusions.

II. THEORY

We consider a homogeneous and isotropic ensemble with $N \gg 1$ spheres, N_β of them with radius a_β, located at random positions $\{R_i^\beta\}$, within a homogeneous medium with dielectric function ϵ_h. All the spheres are made of the same material and are characterized by the dielectric function $\epsilon_s^\beta(\omega)$. The system is excited by a position-dependent external field $\mathbf{E}^{ex}$ oscillating at frequency ω and with wavelength much greater than the radii of the spheres and the typical separation between them. In the quasistatic-dipolar approximation the induced dipole moment $\mathbf{p}_i^\beta$ of the ith sphere with radii a_β is given by

$$\mathbf{p}_i^\beta = \alpha_\beta(\omega) \left[\mathbf{E}_{i,\beta}^0(\omega) + \sum_{j,\gamma} \overset{\leftrightarrow}{\mathbf{t}}_{ij}^{\beta\gamma} \cdot \mathbf{p}_j^\gamma \right], \tag{1a}$$

where

$$\alpha_\beta(\omega) = a_\beta^3 (\epsilon_s^\beta - \epsilon_h)/(\epsilon_s^\beta + 2\epsilon_h) \tag{1b}$$

is the effective polarizability of the spheres with radius a_β, $\mathbf{E}_{i,\beta}^0$ is the induced field at $\mathbf{R}_i^\beta$ in the absence of the spheres, and

$$\overset{\leftrightarrow}{\mathbf{t}}_{ij}^{\beta\gamma} \equiv (1 - \delta_{ij}\delta_{\beta\gamma})\nabla_i\nabla_j(1/R_{ij}^{\beta\gamma}) \tag{1c}$$

is the dipole-dipole interaction tensor. Here $R_{ij}^{\beta\gamma} = |\mathbf{R}_i^\beta - \mathbf{R}_j^\gamma|$ and Greek indices distinguish between spheres with different radii.

The polarization field $\mathbf{P}$ of the system is given by

$$\mathbf{P}(\mathbf{r}) = \left\langle \sum_{i,\gamma} \mathbf{p}_i^\gamma \delta(\mathbf{r} - \mathbf{R}_i^\gamma) \right\rangle, \tag{2}$$

where $\langle \ \rangle$ means ensemble average.

The effective (or macroscopic) dielectric response ϵ_M of the composite is then obtained through[15]

$$\frac{\epsilon_h(\omega)}{\epsilon_M(\omega)} = 1 - 4\pi\epsilon_h \chi^{ex,l}(q \to 0, \omega), \tag{3a}$$

where $\chi^{ex,l}$ is the longitudinal projection of the Fourier transform of the external susceptibility, defined as

$$\mathbf{P}(\mathbf{q},\omega) = \overset{\leftrightarrow}{\chi}^{ex}(\mathbf{q},\omega) \cdot \mathbf{E}^{ex}(\mathbf{q},\omega) \tag{3b}$$

and $\mathbf{q}$ is the wave vector. We remark that the introduction of the wave vector $\mathbf{q}$ eliminates the conditional convergence problems and the shape dependence of some dipolar sums that appear in the theory for constant external fields, when the thermodynamic limit is taken first, and the $q \to 0$ limit is taken afterwards.[15]

Since there is no longitudinal-transverse coupling on a macroscopic scale, due to the symmetry properties of the ensemble, in order to calculate $\chi^{ex,l}(q \to 0, \omega)$ it is sufficient to excite the system with a longitudinal external field with a single Fourier component, that is

$$\mathbf{E}^{ex}(\mathbf{r}) = \hat{\mathbf{q}} E^{ex}(\omega) e^{i\mathbf{q}\cdot\mathbf{r}}. \tag{4}$$

Substituting Eq. (4) into Eq. (1) we can write

$$\mathbf{P}_i^\beta = \alpha_\beta \left[\hat{\mathbf{q}} E^{ex}/\epsilon_h + \sum_{j,\gamma} \overset{\leftrightarrow}{\mathbf{T}}_{ij}^{\beta\gamma} \cdot \langle \mathbf{P}^\gamma \rangle \right.$$
$$\left. + \sum_{j,\gamma} \overset{\leftrightarrow}{\mathbf{T}}_{ij}^{\beta\gamma}(\mathbf{P}_j^\gamma - \langle \mathbf{P}^\gamma \rangle) \right], \tag{5a}$$

where we define

$$\mathbf{P}_i^\beta = \mathbf{p}_i^\beta e^{-i\mathbf{q}\cdot\mathbf{R}_i^\beta}, \tag{5b}$$

$$\overset{\leftrightarrow}{\mathbf{T}}_{ij}^{\beta\gamma} = \overset{\leftrightarrow}{\mathbf{t}}_{ij}^{\beta\gamma} e^{-i\mathbf{q}\cdot(\mathbf{R}_i^\beta - \mathbf{R}_j^\gamma)}, \tag{5c}$$

in order to get rid of the trivial exponential factors; the explicit dependence on $\mathbf{q}$ and ω has been omitted. Notice that we have separated the contribution of the dipolar fluctuations in the last term of the right-hand side of Eq. (5a) and that the average of $\mathbf{P}_i^\gamma$ is independent of i due to homogeneity of the ensemble.

The Fourier transform of the polarizability field is then given by

$$\mathbf{P}(q) = \frac{1}{V} \sum_{i,\gamma} \mathbf{P}_i^\gamma(q) = \sum_\gamma n_\gamma \langle \mathbf{P}^\gamma \rangle(q) \ , \tag{6}$$

where n_γ is the number density of spheres of radius γ, V is the volume of the system, and we have assumed that the spatial and ensemble average are identical due to the homogeneity of the system.

Following the same procedure as in Ref. 15, we take into account the contribution of the dipolar fluctuations through a set of scalar parameters $\{\alpha_\beta^*\}$ which play the role of renormalized polarizabilities, and are defined as

$$\mathbf{P}_i^\beta = \alpha_\beta^* \left[\hat{\mathbf{q}} E^{ex}/\epsilon_h + \sum_{j,\gamma} \overleftrightarrow{\mathbf{T}}_{ij}^{\beta\gamma} \cdot \langle \mathbf{P}^\gamma \rangle \right] \ . \tag{7}$$

Taking longitudinal projection, ensemble average, and the $q \to 0$ limit on both sides of Eq. (7), it is easily shown that

$$\langle P^{\beta,l} \rangle = \frac{\alpha_\beta^*}{1 + 2f\tilde{\alpha}_{av}^*}(E^{ex}/\epsilon_h) \ , \tag{8a}$$

where the superscript l means longitudinal projection and

$$f\tilde{\alpha}_{av}^* = \sum_\gamma f_\gamma \tilde{\alpha}_\gamma^* \ . \tag{8b}$$

Here, f is the volume fraction of the spheres, $f_\gamma = 4\pi a_\gamma^3 n_\gamma/3$ is the volume fraction of spheres of radius a_γ, $\tilde{\alpha}_\gamma^* = \alpha_\gamma^*/a_\gamma^3$, and we have used the result

$$\lim_{q \to 0} \left\langle \sum_{j,\gamma} T_{ij}^{\beta\gamma,l}(q) \right\rangle = -\frac{8\pi}{3} n_\beta \ . \tag{9}$$

Using Eqs. (8a), (6), and (3) we are able to write finally

$$\frac{\epsilon_M(\omega)}{\epsilon_h(\omega)} = \frac{1 + 2f\tilde{\alpha}_{av}^*}{1 - f\tilde{\alpha}_{av}^*} \tag{10}$$

which has the same functional form as MGT but with $f\tilde{\alpha}$ replaced by $f\tilde{\alpha}_{av}^*$. In the absence of the renormalization

procedure $f\tilde{\alpha}_{av}^* = f\tilde{\alpha}_{av} = f\tilde{\alpha}$, one recovers MGT and there is no effect coming from polydispersion.

In order to calculate $\tilde{\alpha}_\gamma^*$ in the most simple way, self-consistency is imposed by substituting Eq. (7) into the right-hand side of Eq. (5a),

$$\mathbf{P}_i^\beta = \alpha_\beta \left[\hat{\mathbf{q}} E^{ex}/\epsilon_h + \sum_{j,\gamma} \overleftrightarrow{\mathbf{T}}_{ij}^{\beta\gamma} \cdot \alpha_\gamma^* \left[\hat{\mathbf{q}} E^{ex}/\epsilon_h \right. \right.$$
$$\left. \left. + \sum_{k,\eta} \overleftrightarrow{\mathbf{T}}_{jk}^{\gamma\eta} \cdot \langle \mathbf{P}^\eta \rangle \right) \right] \ . \tag{11}$$

Taking now longitudinal projection, ensemble average, and the $q \to 0$ limit on both sides of Eq. (11) and using Eq. (8a) we obtain that the $\{\alpha_\beta^*\}$ are determined through the solution of the following set of coupled second-order algebraic equations:

$$\frac{\alpha_\beta^*}{\alpha_\beta} = 1 + \sum_{\gamma,\eta} \alpha_\gamma^* \alpha_\eta^* \Delta T_{\gamma\eta}^\beta \ , \tag{12a}$$

where

$$\Delta T_{\gamma\eta}^\beta \equiv \left\langle \sum_{j,k} \hat{\mathbf{q}} \cdot \overleftrightarrow{\mathbf{T}}_{ij}^{\beta\gamma} \cdot \overleftrightarrow{\mathbf{T}}_{jk}^{\gamma\eta} \cdot \hat{\mathbf{q}} \right\rangle$$
$$- \left\langle \sum_j \hat{\mathbf{q}} \cdot \overleftrightarrow{\mathbf{T}}_{ij}^{\beta\gamma} \cdot \hat{\mathbf{q}} \right\rangle \left\langle \sum_k \hat{\mathbf{q}} \cdot \overleftrightarrow{\mathbf{T}}_{ik}^{\gamma\eta} \cdot \hat{\mathbf{q}} \right\rangle \tag{12b}$$

is related to the fluctuations of the field. In the case of uncorrelated fluctuations $\Delta T_{\gamma\eta}^\beta = 0$ and one recovers the mean-field MGT. Let us recall that $\Delta T_{\gamma\eta}^\beta$ is independent of i due to the homogeneity of the ensemble.

The calculation of $\Delta T_{\gamma\eta}^\beta$ can be done in terms of the m-particle distribution functions $\rho_{\beta,\gamma,\ldots,\mu}^{(m)} \times (\mathbf{R}_1, \mathbf{R}_2, \ldots, \mathbf{R}_m)$ which are proportional to the probability of finding a sphere of radius α_β at $\mathbf{R}_1$, a sphere of radius a_γ at $\mathbf{R}_2, \ldots$, and a sphere of radius a_μ at $\mathbf{R}_m$. In terms of the two- and three-particle distribution functions, we rewrite Eq. (12b) as

$$a_\gamma^3 a_\eta^3 \Delta T_{\gamma\eta}^\beta = \tfrac{1}{4} f_{\beta\gamma} \delta_{\eta\beta} + \left[\frac{3}{4\pi} \right]^2 f_\gamma f_\eta 2 \int d^3 R_{12} \int d^3 R_{23} \frac{P_2(\hat{\mathbf{R}}_{12} \cdot \hat{\mathbf{R}}_{23})}{R_{12}^3 R_{23}^3} [\rho_{\beta\gamma\eta}^{(3)}(\mathbf{R}_1, \mathbf{R}_2, \mathbf{R}_3) - \rho_{\beta\gamma}^{(2)}(\mathbf{R}_1, \mathbf{R}_2) \rho_{\gamma\eta}^{(2)}(\mathbf{R}_2, \mathbf{R}_3)] \ , \tag{12c}$$

where P_2 is the Legendre polynomial of order 2,

$$f_{\beta\gamma} \equiv \frac{24 f_\gamma}{(1 + a_\gamma/a_\beta)^3} \int_0^\infty \frac{\rho_{\beta\gamma}^{(2)}[(a_\beta + a_\gamma)x]}{x^4} dx \ , \tag{12d}$$

and we choose the normalization

$$\frac{1}{V^{(m-1)}} \int d^3 R_1 \int \cdots \int d^3 R_m \, \rho_{\beta,\gamma,\ldots,\mu}^{(m)}(\mathbf{R}_1, \mathbf{R}_2, \ldots, \mathbf{R}_m) = 1 \ . \tag{13}$$

III. RESULTS

In this section we present numerical results to illustrate the consequences of polydispersion on the macroscopic dielectric response. To that end we make a further ap-

proximation. We notice that the second term on the right-hand side of Eq. (12c) has an explicit quadratic dependence in the volume fractions. Thus, in what follows we keep only the first term on the right-hand side of Eq. (12c), which is valid at low enough densities. Under this simplifying assumption Eq. (12) becomes

$$\frac{\tilde{\alpha}_\beta^*}{\tilde{\alpha}_\beta} = 1 + \tfrac{1}{4} \sum_\gamma f_{\beta\gamma} \tilde{\alpha}_\beta^* \tilde{\alpha}_\gamma^* . \qquad (14)$$

In the case in which the dielectric functions ϵ_s^β of the spheres are all identical, then $\tilde{\alpha}_\beta = (\epsilon_s - \epsilon_h)/(\epsilon_s + 2\epsilon_h)$ is independent of β.

Now, we solve the system of coupled quadratic equations [Eq. (14)] for a specific system. For concreteness we choose the simplest two-particle distribution function

$$\rho_{\beta\gamma}^{(2)}(R) = \Theta(R - (a_\beta + a_\gamma)) , \qquad (15)$$

where Θ is the unit step function. This distribution function, known as the hole correction, takes into account the excluded-volume correlation between spheres of different radii. For applications to real systems one should determine $\rho_{\beta\gamma}^{(2)}$ directly from the samples and it will depend, in general, on the volume fraction of the particles. Our choice here is done only to show the importance of the two-particle correlations in the effective dielectric response of the system; the use of a more realistic two-particle distribution of a polydispersed system[35] will be highly desirable.

We concentrate our attention on the case of metallic spheres embedded in gelatin. The dielectric function of the metallic spheres will be modeled by a Drude dielectric function

$$\epsilon_s(\omega) = 1 - \frac{\omega_p^2}{\omega(\omega + i/\tau)} , \qquad (16)$$

where ω_p is the plasma frequency and τ the electronic relaxation time. For the gelatin we take $\epsilon_h = 2.37$ independent of frequency.

We solve the system of coupled quadratic equations given in Eq. (14) using an iterative procedure. At each step of the iteration we choose the roots with a positive imaginary part and we demand continuity of $\{\tilde{\alpha}_\beta^*\}$ as a function of frequency, partial volume fractions $\{f_\beta\}$, and radii ratios $\{a_\gamma/a_\beta\}$; the effective dielectric function is then given by Eq. (10).

In Fig. 1 we show the imaginary part of $\epsilon_M(\omega)$ calculated with our theory for three different composites with the same total volume fraction $f = \tfrac{1}{10}$. The systems are made of inclusions of only one radius, of inclusions of two radii in the ratio 1:16 with partial volume fractions of $\tfrac{1}{20}$ each, and of inclusions of three different radii in the ratio 1:4:16 with partial volume fractions of $\tfrac{1}{30}$ each. We took the Drude parameter as $\omega_p\tau = 92$, which corresponds to an electron mean free part $l \sim 120$ Å for the case of silver ($\hbar\omega_p = 9.2$ eV and $V_F = 1.39 \times 10^8$ cm/sec). We also show the result of MGT with the same parameters. One can see that the results of our theory differ appreciably from the ones of MGT: They discriminate systems with different radii ratios, the position and height of the main peaks are red shifted and lower, and the curves are asymmetric, broader, and with a richer structure than the Lorentzian corresponding to MGT. As already mentioned in Ref. 15, while in our theory the broadening of the curves is dominated by the excitation of collective electromagnetic modes whose frequencies span a finite range, due to the disorder-induced fluctuations, in MGT
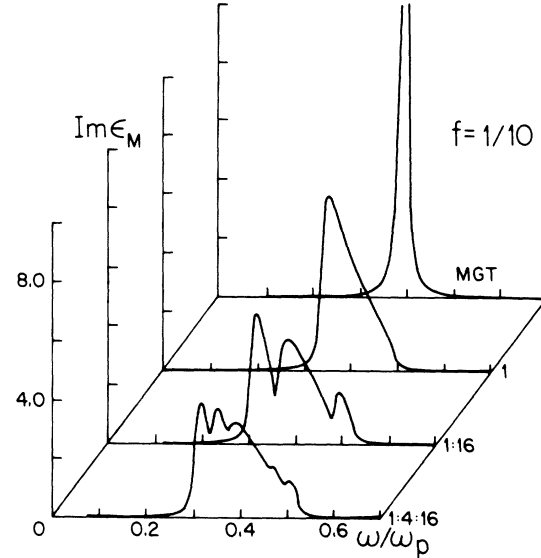

FIG. 1. $\mathrm{Im}\epsilon_M$ as a function of ω/ω_p for a system of Drude spheres with $\omega_p\tau = 92$ and $f = \tfrac{1}{10}$ embedded in gelatin with $\epsilon_h = 2.37$. The curve (MGT) was calculated using MGT and the other three using Eqs. (14), (8), and (10) for spheres (1) with the same radius, (1:16) two different radii in ratio 1:16 and partial volume fractions of $\tfrac{1}{20}$ each, and (1:4:16) three different radii in ratio 1:4:16 and partial volume fractions of $\tfrac{1}{30}$ each.

there is only one log-wavelength optical mode whose broadening is dominated by the value of the electronic relaxation time. Our theory also predicts that as we increase the number of species the main peak shifts to the red and decreases in height while additional structure appears to the right of the main peak. Although the number of peaks increases, they become less pronounced. Therefore one could expect that they will smooth out for a continuous distribution of radii; this is the problem that we now undertake.

We choose a log-normal distribution of radii which is the distribution that has been observed[21,36,37] and predicted[36] for samples prepared through a coalescence mechanism. In a log-normal distribution the number of particles per logarithmic radius interval obeys a normal distribution, and is given by[38]

$$D(R) = \frac{1}{\sqrt{2\pi}} \frac{1}{R \ln\sigma_{NL}} \exp\left[-\frac{1}{2} \left(\frac{\ln(R/R_0)}{\ln\sigma_{NL}} \right)^2 \right] , \qquad (17)$$

where σ_{NL} is a measure of the width of the distribution, R_0 is its median, and $D(R)$ is normalized to unity. The value $\sigma_{NL} = 1$ yields a δ function at R_0 and corresponds to the monodispersed case. In Fig. 2 we show a series of graphs of $D(x) \equiv R_0 D(R)$ as a function of $x \equiv R/R_0$ for several values of σ_{NL}.

In order to calculate ϵ_M we discretize the distribution as follows: we define x_{min} and x_{max} as the extreme values of x such that $D(x) < 0.005$ and we locate a set of p equidistant points $\{x_\gamma\} = \{x_1, x_2, \ldots, x_p\}$ in the interval $[x_{max}, x_{min}]$. We now consider a system of spheres with partial volume fractions $f_\gamma = fx_\gamma^3 D(x_\gamma)/$
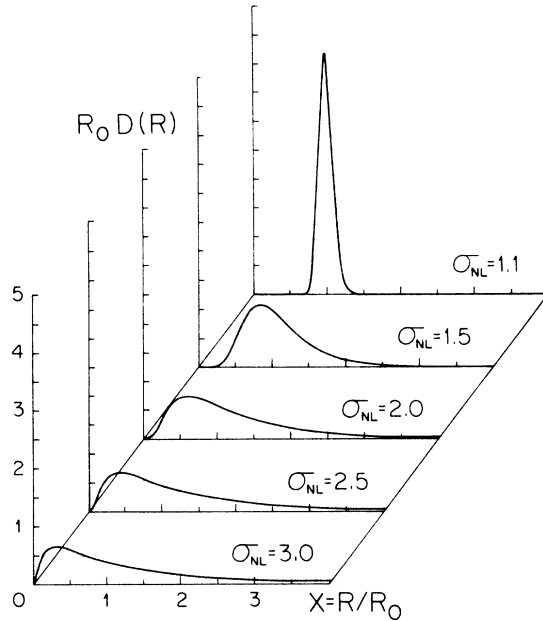
FIG. 2. Log-normal distribution $R_0 D(R)$ as a function of $x = R/R_0$, for different values of $\sigma_{\rm NL}$.

FIG. 3. $\text{Im}\epsilon_M$ as a function of ω/ω_p for a system of Drude spheres embedded in gelatin with $\epsilon_h = 2.37$ and a log-normal distribution of radii for different values of $\sigma_{\rm NL}$. Here, $f = \frac{1}{10}$ and $p = 21$. For each value of $\sigma_{\rm NL}$ curves with three values of $\omega_p \tau$ are displayed. The highest, the middle, and the lowest correspond to $\omega_p \tau = 45$, 82, and 178, respectively. The highest is also the steepest at the low-frequency edge.

$[\sum_{\gamma=1}^{p} x_\gamma^3 D(x_\gamma)]$ and radii $\{a_\gamma\} = \{x_\gamma R_0\}$. The set $\{\tilde{\alpha}_\gamma^*\}$ is then obtained by solving the system of p coupled quadratic equations given by Eq. (14), using the same iterative procedure as before. The limit of a continuous distribution of radii is attained when an increment in p does not change the results.

In Fig. 3 we show the imaginary part of $\epsilon_M(\omega)$ for a system with a log-normal distribution of radii with several $\sigma_{\rm NL}$ and three different relaxation times: $\omega_p \tau = 45$, 82, and 178. The relaxation times are identical in all the spheres and they correspond, in the case of silver, to electronic mean free paths of 50, 100, and 300 Å, respectively. We attained the continuous limit for $p = 21$. The line shapes are asymmetric and there is a main absorption peak with almost no additional structure. As $\sigma_{\rm NL}$ grows the height of the peak diminishes and the absorption frequency range increases. For a given ω_p and a given $\sigma_{\rm NL}$ an increase in τ affects the shape of the curve only in a small region close to the peak and at the absorption edge. On the other hand, MGT generates a Lorentzian curve with a width directly proportional to $1/\tau$ independent of $\sigma_{\rm NL}$. This can be readily understood by analyzing the difference in roles played by the dipolar fluctuations and the electronic relaxation time during the absorption process. This process can be pictured as an accumulation of energy through the excitation of the different electromagnetic normal modes of the system. If the contribution of the dipolar fluctuations is neglected, as in MGT, there is only one optical mode excited and in the absence of any other dissipation processes it shows up in $\text{Im}\epsilon_M$ as a δ function. The introduction of a relaxation time τ opens channels through which the electromagnetic energy accumulated in the normal modes is dissipated into other forms of energy, yielding a finite width proportional to $1/\tau$. In our theory, the contribu-
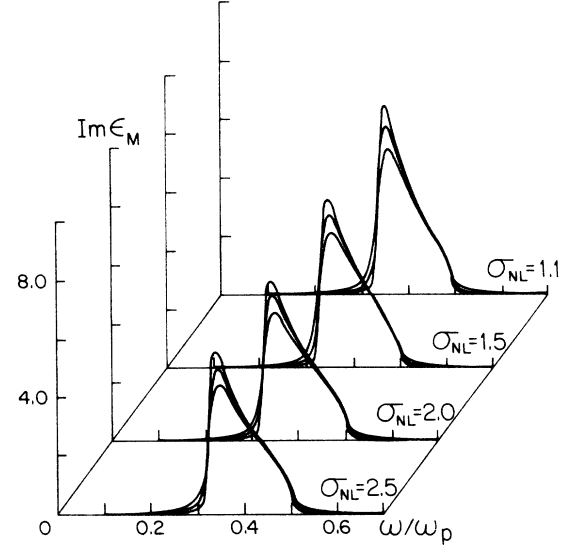
tion of the dipolar fluctuations allows the excitation of a whole collection of electromagnetic modes whose frequencies span a continuous range even when $\tau \to \infty$. Dissipation, introduced through the relaxation time τ, will broaden the contribution of each mode by $\Delta\omega \cong 1/\tau$. For the values of τ chosen here, $\Delta\omega/\omega_p = 0.022$ 0.012, and 0.006. Therefore, a finite value of τ will enlarge slightly the frequency region of absorption by $\sim \Delta\omega$ and will also smooth out any structure narrower than $\Delta\omega$. This can be clearly seen in Fig. 3 where, for all $\sigma_{\rm NL}$, the effect of decreasing τ only affects a small region around the main peak and near the absorption edge.

From the results shown in Fig. 3 one could expect that the inclusion of surface scattering through a size-dependent τ should have only a small influence in $\text{Im}\epsilon_M(\omega)$. This can be shown by taking in Eq. (14)

$$\tilde{\alpha}_\beta = \frac{\epsilon_s(\tau_\beta) - \epsilon_h}{\epsilon_s(\tau_\beta) + 2\epsilon_h} , \qquad (18)$$

where $\epsilon_s(\tau_\beta)$ is given by Eq. (16) but with a size-dependent relaxation time τ_β given by

$$\frac{1}{\tau_\beta} = \frac{1}{\tau_B} + \frac{V_F}{a_\beta} . \qquad (19)$$

Here, V_F is the Fermi velocity, τ_B is the relaxation time in the bulk, and Eq. (19) is the simplest way to incorporate surface scattering.

The calculation of $\text{Im}\epsilon_M(\omega)$ is done using the same procedure as before, that is through the solution of Eq. (14) combined with Eqs. (8b) and (10). In order to be able to compare these results with the ones of Fig. 3, we choose the same system with a log-normal distribution of
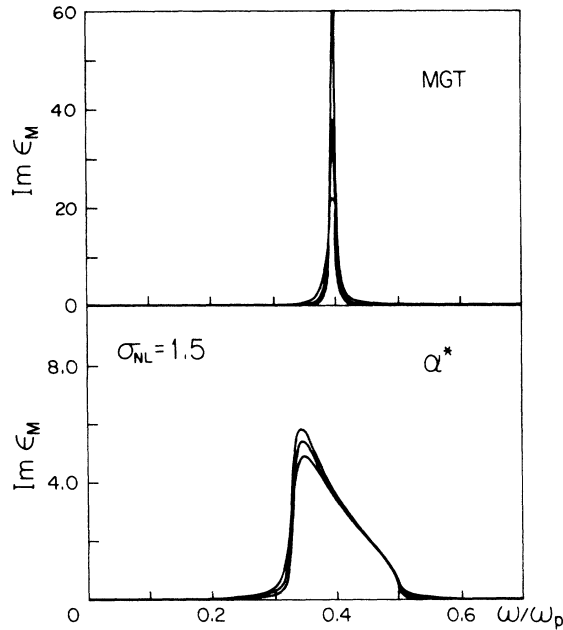
FIG. 4. Upper panel: $\mathrm{Im}\epsilon_M$ as a function of ω/ω_p calculated within MGT for a system of silver spheres embedded in gelatin with $f = \frac{1}{10}$, $\epsilon_h = 2.37$, and a log-normal distribution of radii with $\sigma_{NL} = 1.5$ and $p = 21$. Three curves are displayed for three different values of the median R_0. The highest, the middle, and the lowest correspond to R_0 equal to 50, 100, and 300 Å, respectively. Silver was modeled by a Drude response with τ given by Eq. (19) with $V_F = 1.39 \times 10^8$ cm/sec and $\tau_B = 3.1 \times 10^{-14}$ sec. Lower panel: $\mathrm{Im}\epsilon_M$ as a function of ω/ω_p calculated with Eqs. (14), (8), and (10) for the same system and the same parameters as above.

radii [Eq. (17)] with $\sigma_{NL} = 1.5$, $R_0 = 50$, 100, and 300 Å, and $p = 21$. The results of this calculation are shown in the lower panel of Fig. 4 with $\tau_B = 3.1 \times 10^{-14}$ sec. In the upper panel we display $\mathrm{Im}\epsilon_M(\omega)$ using MGT and the same parameters as above. As it was presumed, while in MGT the width of the absorption peak is governed by the distribution of relaxation times, in our theory it only affects the height of the peak and a small region around it and near the absorption edge.

IV. CONCLUSIONS

We have calculated the effective dielectric response $\epsilon_M(\omega)$ of a composite, within the long-wavelength dipolar approximation, by extending the concept of a renormalized polarizability, introduced in Ref. 15, to a polydispersed system. This renormalized polarizability accounts, in an approximate way, for the dipolar fluctuations, thus it yields a theory which goes beyond mean field. We treated the case of a homogeneous and isotropic ensemble of spherical inclusions with a continuous distribution of radii, immersed in homogeneous medium. A different renormalized polarizability was assigned to each class of spheres characterized by its radius. The statistical properties of the ensemble enter in the final result through the two- and three-particle distribution functions. The calculation was performed for a system of silver spheres embedded in gelatin. The Drude model was used for the dielectric response of silver, the response

for the gelatin was taken independent of frequency, and we neglected the corrections due to three-particle correlations [second term of Eq. (12c)]. We show results for $\mathrm{Im}\epsilon_M(\omega)$ using a log-normal distribution of radii, a size independent relaxation time in the Drude response, and a step function for $\rho_{\alpha\beta}^{(2)}$. They display an asymmetric resonance peak whose broadening is controlled by the spectrum of excitation of the collective electromagnetic modes allowed by the dipolar fluctuations. An increase in the width of the distribution of radii enlarges the broadening and the absorption region. Changes in the values of τ diminish the height of the peak but they have only a slight influence outside a region of order $\Delta\omega = 1/\tau$ around the peak. The inclusion of surface scattering through a distribution of relaxation times does not produce a substantial change in our results. This contrasts with MGT, where the broadening of the absorption peak is determined solely by the distribution of relaxation times.

There have been other calculations beyond mean field for a polydispersed system.[2,6,13] Some of them[2,6] were done by simulating the spatially disordered system by a cubic crystal with a collection of spheres randomly located within the unit cell and then the results were averaged over many configurations. In these calculations neither the distribution of radii nor the two-particle distribution function were reported, thus adequate comparison with our theory was not possible. The case of two different radii has been treated by Liebsch and Villaseñor[8] within the lattice-gas coherent-potential approximation (LG-CPA) and, as already pointed out in Ref. 34, we found a discrepancy with our results. While we obtained a large red shift of the absorption peak by increasing the radius ratio, LG-CPA gave a slight blue shift. Taking into consideration that in LG-CPA the spheres are located at the lattice points of a cubic lattice, when spheres of two different sizes occupy the lattice, the small spheres will be artificially separated from the large ones and from each other. We have repeated our calculation for the case of two different radii but now choosing a two-particle distribution function $\rho_{\alpha\beta}^{(2)}$ which could simulate this effect. We took for all pairs of particles $\rho_{\alpha\beta}^{(2)}(R) = \Theta(R - 2A)$, where A is the radius of the large particle and we obtained a blue shift with a similar behavior as in LG-CPA. This shows the importance of the two-particle distribution function as a necessary input in the calculation of the effective dielectric response of a composite. Unfortunately this type of information has only recently been reported along with the experimental results.[39] Nevertheless a careful analysis of the dependence of our results with a more realistic two-particle distribution function of a polydispersèd system (i.e., within the Percus-Yevick approximation[35] would be highly desirable. Also, the inclusion of the effects of the three-particle correlation functions are indispensable to extend this calculation to higher volume fractions.

[1]R. Fuchs, in *Electrical, Transport and Optical Properties of Inhomogeneous Media,* AIP Conf. Proc. No. 40, edited by J. C. Garland and D. B. Tanner (AIP, New York, 1978), p. 278.

[2]W. Lamb, D. M. Wood, and N. W. Ashcroft, Phys. Rev. B **21**, 2248 (1980).

[3]P. Sheng, Phys. Rev. Lett. **45**, 60 (1980).

[4]G. A. Niklasson, C. G. Granqvist, and O. Hunderi, Appl. Opt. **20**, 26 (1981).

[5]J. M. Gerardy and M. Ausloss, Phys. Rev. B **26**, 4703 (1982).

[6]Y. Kantor and D. J. Bergman, J. Phys. C **15**, 2033 (1982).

[7]B. N. J. Persson and A. Liebsch, Solid State Commun. **44**, 1637 (1982); A. Liebsch and B. N. J. Persson, J. Phys. C **16**, 5373 (1983).

[8]A. Liebsch and P. Villaseñor-González, Phys. Rev. B **29**, 6907 (1984).

[9]M. Gómez, L. Fonseca, G. Rodríguez, A. Velázquez, and L. Cruz, Phys. Rev. B **32**, 3429 (1985).

[10]R. Rojas and F. Claro, Phys. Rev. B **34**, 3730 (1986).

[11]V. A. Davis and L. Schwartz, Phys. Rev. B **31**, 5155 (1985); **33**, 6627 (1986).

[12]S. Torquato and F. Lado, Phys. Rev. B **33**, 6428 (1986).

[13]B. U. Felderhof and R. B. Jones, Z. Phys B **62**, 43 (1986); **62**, 215 (1986); **62**, 225 (1986); **62**, 231 (1986).

[14]E. Martina, *Electrodynamics of Interfaces and Composite Systems,* Vol. 4 of *Advanced Series in Surface Science,* edited by R. G. Barrera and W. L. Mochán (World Scientific, Singapore, 1988), p. 492.

[15]R. G. Barrera, G. Monsivais, and W. L. Mochán, Phys. Rev. B **38**, 5371 (1988).

[16]G. F. Dell'Antonio and V. Nesi, J. Math. Phys. **29**, 2688 (1988).

[17]R. H. Doremus, J. Chem. Phys. **40**, 2389 (1964); **42**, 414 (1965); J. Appl. Phys. **37**, 2775 (1966).

[18]R. W. Cohen, G. D. Cody, M. D. Coults, and B. Abelès, Phys. Rev. B **8**, 3689 (1973).

[19]E. B. Priestley, B. Abelès, and R. W. Cohen, Phys. Rev. B **12**, 2121 (1975).

[20]J. I. Gittleman and B. Abelès, Phys Rev. B **15**, 3273 (1977).

[21]C. G. Granqvist and O. Hunderi, Phys. Rev. B **16**, 3513 (1977).

[22]T. Welker and T. P. Martin, J. Chem. Phys. **70**, 5683 (1979).

[23]U. Kreibig, A. Althoff, and H. Pressman, Surf. Sci. **106**, 308 (1981).

[24]U. J. Gibson, H. G. Craighead, and R. A. Buhrman, Phys. Rev. B **25**, 1449 (1982).

[25]K. D. Cummings, J. C. Garland, and D. B. Tanner, Phys. Rev. B **30**, 4170 (1984).

[26]G. A. Niklasson and C. G. Granqvist, J. Appl. Phys. **55**, 3382 (1984).

[27]W. J. Kaiser, E. M. Logothetis, and L. E. Wenger, Solid State Commun. **58**, 83 (1986); J. Phys. C **18**, L837 (1985).

[28]S. I. Lee, T. W. Noh, J. R. Gaines, Y. H. Ko, and E. R. Kreidler, Phys. Rev. B **37**, 2918 (1988).

[29]See U. Kreibig, J. Phys. F **4**, 999 (1974), and references therein.

[30]U. Kreibig, Z. Phys. B **31**, 39 (1978).

[31]Yu. E. Lozovik and V. N. Nishanov, Fiz. Tverd. Tela (Leningrad) **20**, 3654 (1978) [Sov. Phys.—Solid State **20**, 2111 (1979)]; A. Kawabata and R. Kubo, J. Phys. Soc. Jpn. **21**, 1765 (1966); A. A. Lushnihov and A. J. Simonov, Z. Phys. **270**, 17 (1974); L. Genzel, T. P. Martin, and U. Kreibig, Z. Phys. B **21**, 339 (1975); H. Abe, W. Shulze, and B. Tesche, Chem. Phys. **47**, 95 (1980); D. B. Tran Thoai and W. Ekardt, Solid State Commun. **41**, 687 (1982); D. M. Wood and N. W. Ashcroft, Phys. Rev. B **25**, 6255 (1982); W. Ekardt, *ibid.* **31**, 6360 (1985); **34**, 526 (1986).

[32]See, for example, C. F. Bohren and D. R. Huffman, *Absorption and Scattering of Light by Small Particles* (Wiley, New York, 1983), p. 79.

[33]See, for example, Refs. 14, 15, 18, 19, and 22.

[34]R. G. Barrera, P. Villaseñor-González, W. L. Mochán, M. del Castillo-Mussot, and G. Monsivais, Phys. Rev. B **39**, 3522 (1989).

[35]See, for example, J. L. Lebowitz, Phys. Rev. **113**, A895 (1964); N. W. Ashcroft and D. C. Langreth, *ibid.* **156**, 685 (1967); L. Blum and G. Stell, J. Chem. Phys. **71**, 42 (1979); P. J. Leonard, D. Henderson, and J. A. Barker, Mol. Phys. **21**, 107 (1971).

[36]C. G. Granqvist and R. A. Buhrman, Appl. Phys. Lett. **27**, 693 (1975); J. Appl. Phys. **47**, 2200 (1976).

[37]G. H. Comsa, J. Phys. (Paris) Colloq. **38**, C2-185 (1977).

[38]J. Aitchison and J. A. C. Brown, *The Lognormal Distribution* (Cambridge University Press, Cambridge, England, 1957).

[39]G. A. Niklasson, Solar Energy Mater. **17**, 217 (1988).